

Improving of Anticancer Activity and Solubility of Cisplatin by Methylglycine and Methyl Amine Ligands Against Human Breast Adenocarcinoma Cell Line

Fatemeh Safa Shams Abyaneh¹ ·
Mahboube Eslami Moghadam² · Adeleh Divsalar³ ·
Davood Ajloo⁴ · Moyaed Hosaini Sadr¹

Received: 15 November 2017 / Accepted: 6 February 2018
© Springer Science+Business Media, LLC, part of Springer Nature 2018

Abstract Methylglycine, also known sarcosine, is dramatically used in drug molecules and its metal complexes can interact to DNA and also do cleavage. Hence, to study the influence of methylglycine ligand on biological behavior of metal complexes, two water-soluble platinum (II) complexes with the formula $\text{cis-}[\text{Pt}(\text{NH}_3)_2(\text{CH}_3\text{-gly})]\text{NO}_3$ and $\text{cis-}[\text{Pt}(\text{NH}_2\text{-CH}_3)_2(\text{CH}_3\text{-gly})]\text{NO}_3$ (where $\text{CH}_3\text{-gly}$ is methylglycine) have been synthesized and characterized by spectroscopic methods, molar conductivity measurements, and elemental analyzes. The anticancer activity of synthesized complexes was tested against human breast adenocarcinoma cell line of MCF7 using MTT assay and results showed excellent anticancer activity with C_{50} values of 126 and 292 μM after 24 h incubation time, for both complexes of $\text{cis-}[\text{Pt}(\text{NH}_3)_2(\text{CH}_3\text{gly})]\text{NO}_3$ and $\text{cis-}[\text{Pt}(\text{NH}_2\text{-CH}_3)_2(\text{CH}_3\text{gly})]\text{NO}_3$, respectively. Also, the interaction between Pt(II) complexes with calf thymus DNA was extensively studied by means of absorption spectroscopy, fluorescence titration spectra displacement with ethidium bromide (EtBr), and circular dichroism studied in Tris-buffer. The obtained spectroscopic results revealed that two complexes can bind to highly polymerized calf thymus DNA cooperatively and denature at micromolar concentrations. The fluorescence data indicate that quenching effect for $\text{cis-}[\text{Pt}(\text{NH}_3)_2(\text{CH}_3\text{gly})]\text{NO}_3$ ($K_{\text{sv}} = 9.48 \text{ mM}^{-1}$) was higher than that of $\text{cis-}[\text{Pt}(\text{NH}_2\text{-CH}_3)_2(\text{CH}_3\text{gly})]\text{NO}_3$ ($K_{\text{sv}} = 1.98 \text{ mM}^{-1}$). These results were also confirmed by circular dichroism spectra. Consequently, docking data showed that $\text{cis-}[\text{Pt}(\text{NH}_3)_2(\text{CH}_3\text{gly})]\text{NO}_3$ with

✉ Mahboube Eslami Moghadam
eslami_moghadam@ccerci.ac.ir; eslami_moghadam@yahoo.com

¹ Department of Chemistry, Science and Research branch, Islamic Azad University, Tehran, Iran

² Chemistry & Chemical Engineering Research Center of Iran, Tehran, Iran

³ Department of Cell & Molecular Sciences, Faculty of Biological Sciences, Kharazmi University, Tehran, Iran

⁴ School of Chemistry, Damghan University, Damghan, Iran

more interaction energy binds on DNA via groove binding which is more compatible with experimental results.

Keywords Cisplatin analog · Anticancer drug · Cytotoxicity · Methylglycine · DNA interaction · Thermodynamic parameters · Molecular docking

Abbreviations

CT-DNA	Calf thymus DNA
Methylgly	Methyl glycine
CD	Circular dichroism
EB	Ethidium bromide

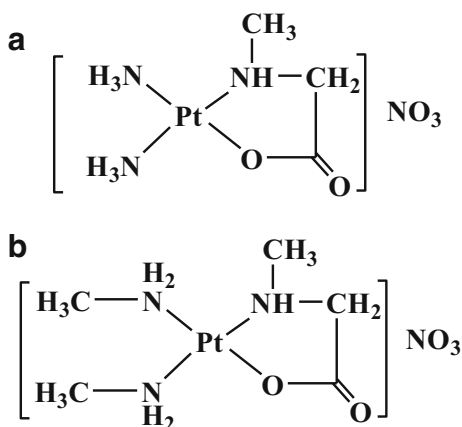
Introduction

Cisplatin, Cis-[Pt(NH₃)₂Cl₂] has been widely used as anticancer drugs for treatment of testicular and solid malignancies like bone, neck, and bladder cancer [1]. Due to the dose limiting toxic side effects of cisplatin, much current research work is aimed at the discovery and design of new platinum complexes which are not cross-resistant with cisplatin and have also fewer toxic side effects and natural clinical activity against a broad range of types of cancer [2, 3]. However, an effective oral formulation of cisplatin is not always achievable because of its poor water solubility and low level of bioavailability of attached ligands [4]. For overcoming the severe side effects and improve clinical effectiveness, the Pt(II) compounds should be tailored to meet the various requirements such as water solubility, chemical stability, biodegradability, and tumor targeting [5]. So, with choosing an appropriate attached ligand sphere, activity of the drugs should be increased, where as it is acceptable to decreased their general toxicity [6].

Hence, amino acids are the fundamental material of life and the basis of metabolism [7]. Introducing amino acid into an antitumor drug can improve selectivity to tumor cells, enhance their liposolubility, and remit their toxicity to normal cells [8]. Indeed, certain tumors and cancer cells are unable to produce all the synthesized amino acids by the normal cells. Therefore, these cells require an external supply of such essential amino acids to pass on to the cancer cells by the blood stream [9]. Furthermore, the amino acids especially the first of them, glycine are very important compounds for the transfer inside the cell of biologically active alkylating agents [10]. In the recent past, numerous of studies have widely used the glycine ligand in the synthesis of Pt(II) complexes and their structure has highlighted in various significant applications [11–13].

In the present work, design, synthesis, and characterization of two new cationic cisplatin analog (see Scheme 1) were bearing with glycine amino acid derivative as chelating ligands are reported [14]. The biological activity of two synthesized Pt complexes were tested against the human breast adenocarcinoma cancer model cell line of MCF7 and showed excellent cytotoxicity effects at micromolar concentration. The binding mechanism of these water-soluble Pt(II) complexes with calf thymus DNA under simulated physiological conditions (pH 7.4) has also been investigated by various spectroscopic techniques including UV-Vis spectroscopy, fluorescence measurements and circular dichroism. Moreover, to quantitatively analyze the interaction of Pt complex DNA, the relative thermodynamic characteristics were investigated. Theoretical methods such as computer simulations and docking could be

Scheme 1 Proposed structure of **a** cis-[Pt(NH₃)₂(CH₃-gly)]NO₃ and **b** cis-[Pt(NH₂-CH₃)₂(CH₃-gly)]NO₃



examined the interactions and described important features for DNA complex recognition. So, binding affinities of the new complexes interactions were also estimated by docking calculations [15].

Experimental Procedures

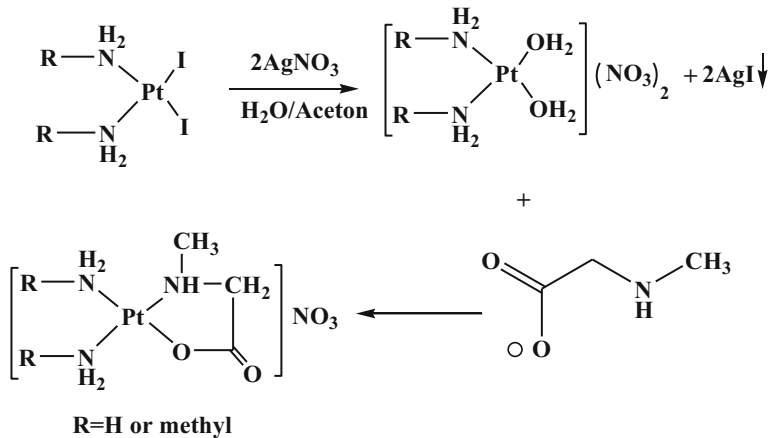
Highly polymerized calf thymus DNA sodium salt and Tris-HCl (tris (hydroxymethyl) amino methane hydrochloride) were purchased from Aldrich Co. (England). Acetone, ethanol, and anhydrous ether, methyl amine and potassium tetrachloride palatinate, barium chloride, sodium chloride, sodium bicarbonate, sodium hydroxide, hydrochloric acid, sulfuric acid, and silver nitrate were purchased from Merck Co. (Germany) used for synthesis complexes. Moreover, methylglycine ligand was made according to the procedure previously described [14].

Spectra of ¹H NMR were recorded using a Bruker Avance spectrometer at 300 MHz, using DMSO-d₆ as the solvent and TMS as the internal reference. Infrared spectra of these complexes were determined on a Perkin Elmer-10.20.00 plus FT-IR spectrophotometer in the range of 400–4000 cm⁻¹ in KBr pellets. UV-Vis spectra were recorded on SPEKOL 2000 spectrophotometer. Conductivity of the synthesized complexes was measured on a Metrohm-712 conduct meter, using water as the solvent. Elemental analysis of carbon, hydrogen, and nitrogen was carried out on an elemental analysis of CHN Rapid Heraeus. Circular dichroism measurements were recorded on an Aviv-215 spectrophotometer and fluorescence measurements were carried out with a JASCO FP- 6500 spectrophotometer.

Synthesis of Pt(II) Complexes

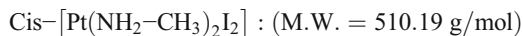
Preparation of two new platinum complexes was described as follow (Scheme 2):



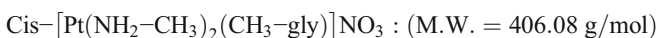


Scheme 2 Schematic reaction of synthesis of two new Pt complexes: cis-[Pt(NH₃)₂(CH₃-gly)]NO₃ and cis-[Pt(NH₂-CH₃)₂(CH₃-gly)]NO₃

This complex was synthesized by [Pt(NH₃)₂I₂] made according to the reported method [16]. One hundred milligrams [Pt(NH₃)₂I₂] (0.2 mmol) and 67 mg AgNO₃ (0.4 mmol) were dissolved and refluxed in 120 mL of double distilled water/acetone (1/3, v/v). The mixture reaction was refluxed at 50 °C for 24 h and string continued for 12 h at room temperature under darkness. After filtering the suspension and removing the AgI precipitate, aqua solution was mixed with 25 mg methylglycine (0.2 mmol) and 33 mg NaHCO₃ (0.4 mmol) dissolved in 10 mL distilled water at 40 °C. Then, the solution was evaporated and concentrated to 5 mL at 35 °C. The brown precipitate was formed and washed with distilled water and acetone and dried in a vacuum oven at room temperature. The yield of reaction was 51%. Analytical calculated for C₃H₁₁N₄O₅Pt compound (378.08) is C, 9.52; H, 2.9; N, 14.81%. Analytical found: C, 9.83; H, 2.57; N, 14.59%. UV Band maxima in nanometer (M in liter mol⁻¹ cm⁻¹ × 10⁻⁴): 200 (29.1). Molar conductance, M (10⁻⁴ M, H₂O): 162.4 Ω⁻¹ cm² mol⁻¹. IR (cm⁻¹, KBr disk): 3419 (s, N-H), 2968 (w, C-H), 1630 (s, C=O), 1381 (s, (NO₃)⁻), ¹H NMR (300 MHz, DMSO-d₆, δ in ppm): 2.6345 (s, 2H), 1.64 (m, 4H), 1.21(m, 4H), 2.9(m, 7H_{NH}).



41.5 mg (0.1 mmol) K₂PtCl₄ was dissolved in 200 μl double distilled water and then 100 mL solution of 0.1 g KI (0.6 mmol) was added to dark red of K₂PtCl₄ solution, the mixture was stirred continuously at 35 °C for 1 h until dark brownish red appeared. Thirty microliters (0.2 mmol) methyl amine was added drop wise to the following solution. The light yellow precipitates were filtered and washed with a small volume of ice water and acetone, respectively. The formed cis-[Pt(NH₂-CH₃)₂I₂] was dried at vacuum oven for 1 day. The yield of synthesis reaction was 73%. IR (cm⁻¹, KBr disk): 3213 (s, N-H), 2955 (s, C-H).



One hundred milligrams cis-[Pt(NH₂-CH₃)₂I₂] (0.195 mmol) was suspended in 120 mL of double distilled water/acetone (1/3, v/v). The solution of 66 mg of AgNO₃ (0.39 mmol) in 10 mL water was added slowly to this suspension with continuous stirring. The reaction mixture was refluxed at 50 °C for 24 h and cooled at the room temperature for 12 h under

darkness. Then, the mixture was filtered to remove gray AgI precipitate by centrifugation. This filtrated solution was mixed with 24 mg synthesized methylglycine hydrochloride (0.1 mmol) and 32 mg NaHCO₃ (0.39 mmol) dissolved in 5 mL distilled water. The reaction mixture was further stirred at 45 °C for 3 h. The reaction mixture was concentrated to 1 mL until the white precipitate was formed. The product obtained was filtered and washed with small amounts of chilled distilled water and acetone and dried in a desiccator. The reaction yield of complex was 51%.

Analytical calculated for C₅H₁₅N₄O₅Pt compound (406.08) is C, 14.77; H, 3.69; N, 13.79%. Analytical found: C, 14.65; H, 3.77; N, 13.59%. UV Band maxima in nanometer (ϵ in liter mol⁻¹ cm⁻¹ × 10⁻⁴): 205 (29.8). Molar conductance, M (10⁻⁴ M, H₂O): 178.5 Ω⁻¹ cm² mol⁻¹. IR (cm⁻¹, KBr disk): 3204 (s, N-H), 3121 (s, C-H), 1606 (s, C=O), 1360 (s, (NO₃)⁻), ¹H NMR (300 MHz, DMSO-d₆, δ in ppm): 2.21 (m, 9H), 2.24 (m, 2H), 5.3729 (m, 5H_{NH}).

In Vitro Cytotoxicity Studies

Cell Culture

Human breast cancer cell line of MCF7 was purchased from the National Cell Bank of Iran (NCBI), Pasteur Institute of Iran. The cells were grown on the DMEM medium (Sigma) supplemented with L-glutamine (2 mM), streptomycin, penicillin (5 µg/ml), and 10% heat-inactivated fetal calf serum at 37 °C under a 5% CO₂/95% air atmosphere.

Cell Proliferation Assay

The anticancer and antiproliferative activity of the designed Pt(II) complexes was measured by MTT assay. The cleavage and conversion of the soluble yellowish MTT to the insoluble purple formazan by active mitochondrial dehydrogenase of living cells have been used to develop an assay system alternative to other assays for measurement of cell proliferation. The harvested cells were seeded into a 96-well plate (1 × 10⁴ cell/ml) and were left to adhere overnight. Prior to the experiments, the cells were twice washed with phosphate-buffered saline (PBS). Then, the MCF7 cancer cells were incubated with different concentrations of sterilized both of the Pt(II) complexes (0–350 µM) and incubated for 24 h. Four hours to the end of the incubation, 25 µL of the MTT solution (5 mg/ml in PBS) was added to each well containing fresh and cultured media. At the end, the insoluble formazan produced was dissolved in a solution containing 10% SDS and 50% DMF (left for 2 h at 37 °C in darkness) and optical density (OD) was read against reagent blank with multi-well scanning spectrophotometer (ELISA reader, Model Expert 96, Asys Hitech, Austria) at the wavelength of 570 nm. The OD value of the study groups was divided by the OD value of the untreated control and presented as the percentage of control (as 100%).

Metal Complexes Interaction with Calf Thymus DNA

Absorption spectroscopy is one of the most commonly useful techniques to study interaction of any metal/drug to CT-DNA [17]. The application of UV absorption is based on monitoring the difference absorption changes upon addition of platinum (II) complexes. The stock solution of DNA was prepared by dissolving 4 mg of DNA in 20 mL Tris-buffer as accordance

to the reports. Here, due to no absorption for Pt complexes in UV-Vis range, the ΔA s for each titration of metal complex was recorded at λ_{\max} (258 nm) of DNA [18].

UV-Vis Spectroscopic Experiment of DNA Denaturation

In this experiment, the reference cell was filled with 1.8 mL Tris-buffer and sample cell was filled with 1.8 mL DNA (0.08 mM). Both cells were settled at constant temperature of 300 and 310 K which were separately titrated with various concentrations of each platinum (II) complex. After 1 min, the absorption was recorded at 258 nm for DNA and at 640 nm to eliminate the interference of turbidity. The injection of metal complex to both cells was continued until no further changes in the absorption readings were observed; these absorption readings of DNA solution were plotted separately versus different concentrations of each metal complex. Thermodynamic parameters like molar Gibbs free energy (ΔG°), molar enthalpy (ΔH°), and molar entropy of DNA binding with complex (ΔS°) were obtained by using the Pace method. The application of UV absorption method to the study of interaction of DNA with Pt(II) complex is similar to that reported earlier [19].

Thermal Denaturation Studies

Sequence differences between two different DNA sequences can also be detected by using DNA denaturation. DNA is heated and denatured into single-stranded state, and the mixture is cooled to permit strands to rehybridize. This experiment was contested in to Tris-buffer using continues heating from 25 to 100 °C. The growth in the temperature was ~ 2 °C/min. The change of absorbance difference was recorded at 258 nm. Since examined, the profile of absorbance agent temperature is almost linear in the melting temperature [20].

Fluorescence Quenching Studies

A quantitative analysis affinity of the Pt(II) complexes was bound to DNA was carried out by luminescence titration method with JASCO spectrofluorimeter (FP6200). A fixed solution of DNA ($60 \mu\text{mol L}^{-1}$) and ethidium bromide ($2 \mu\text{mol L}^{-1}$) was titrated by various concentrations of each Pt complex (50, 100, 150, 200, 250, 300, 350, and $400 \mu\text{mol L}^{-1}$). The emission spectra for both Pt(II) complexes were recorded between 540 and 700 nm with excitation wavelength at 471 nm. The fluorescence intensities of Pt(II) complexes at 471 nm excitation wavelength have been checked which was small and negligible. This experiment, fluorescence emission spectra of intercalated ethidium bromide with increasing of each Pt(II) complexes, was observed [21, 22].

Circular Dichroism Studies

Positive band of DNA due to base stacking (273 nm) and negative one due to right-handed helicity (246 nm) are quite sensitive to interaction mode of DNA small molecules [23]. So, CD spectroscopy is a worthwhile tool to diagnose change in DNA morphology during drug-DNA interactions. CD measurements were conducted on JASCO (J-810) spectropolarimeter by keeping the concentration of DNA constant (5×10^{-5} M) while varying the complex concentration from 0.48 to 1.09 mM at room temperature [24].

Docking Studies

AutoDock 4.2 program was used to obtain the energetic and binding site for the interaction of the titled complexes with DNA. Docking simulation was done in a box with dimension of $52 \times 100 \times 80$ points and the spacing of 0.375 (maximum number of generations and energy evaluation were set to 27,000 and 2.5×10^5 , respectively. For each run, 250 docking energies were reported with the initial population of 250 individuals [25].

Result and Discussion

Determination of the Binding Parameters

Electronic absorption spectroscopy is one of the most important techniques for DNA-binding studies of platinum complexes. The final result of interaction of CT-DNA with cis-[Pt(NH₃)₂(CH₃-gly)]NO₃ and cis-[Pt(NH₂-CH₃)₂(CH₃-gly)]NO₃ are shown in Fig. 1 and summarized in Table 1. DNA denaturation experiment was done by looking at the systematic changes in the UV absorption spectrum of DNA solution at 258 nm upon addition of two platinum complexes. Addition of metal complex and the absorption monitoring was continued until no further changes in the absorption reading were observed at two different temperatures of 300 and 310 K [26]. Some thermodynamic parameters were discussed by using DNA denaturation plots (Fig. 1) and the Pace method. The value of K unfolding equilibrium constant and $\Delta G^\circ_{(H_2O)}$, unfolding of free energy of DNA in the presence of cis-[Pt(NH₃)₂(CH₃-gly)]NO₃ and cis-[Pt(NH₂-CH₃)₂(CH₃-gly)]NO₃ have been calculated by Eqs. (1) and (2) [27], where A_{obs} , A_N , and A_D are the absorbance readings in the transition region, the natural and denatured conformations of DNA, respectively.

$$K = \frac{A_n - A_{obs}}{A_{obs} - A_n} \quad (1)$$

$$\Delta G^\circ = -RT \ln K \quad (2)$$

The straight line is determined when ΔG° are plotted against concentration of cis-[Pt(NH₃)₂(CH₃-gly)]NO₃ and cis-[Pt(NH₂-CH₃)₂(CH₃-gly)]NO₃ in transition region at 300 and 310 K. These plots are shown in Fig. 2. The value of m , that is that is slop of each group in the same plots (a measure of platinum complex ability denature DNA) and intercept of each plot is, ΔG° (conformational stability of DNA in the absence of platinum complexes) [28]. The m value of cis-[Pt(NH₂-CH₃)₂(CH₃-gly)]NO₃ system is higher than those of other Pt(II) complex in room temperature which indicate the much higher ability of cis-[Pt(NH₂-CH₃)₂(CH₃-gly)]NO₃ to denature in 300 K temperature. As we know, the higher value of $\Delta G^\circ_{H_2O}$ indicate a large systematic conformational stability of DNA. However, the value of ΔG° decreases by increasing the temperature for cis-[Pt(NH₂-CH₃)₂(CH₃gly)]NO₃ because most of the macromolecules are less stable at higher temperature. Another important thermodynamics parameter is the molar enthalpy of DNA denaturation in the absence and presence of cis-[Pt(NH₃)₂(CH₃gly)]NO₃ and cis-[Pt(NH₂-CH₃)₂(CH₃gly)]NO₃ complexes. $\Delta H^\circ_{conformational}$ or $\Delta H^\circ_{denaturation}$ is calculated in the range of 300

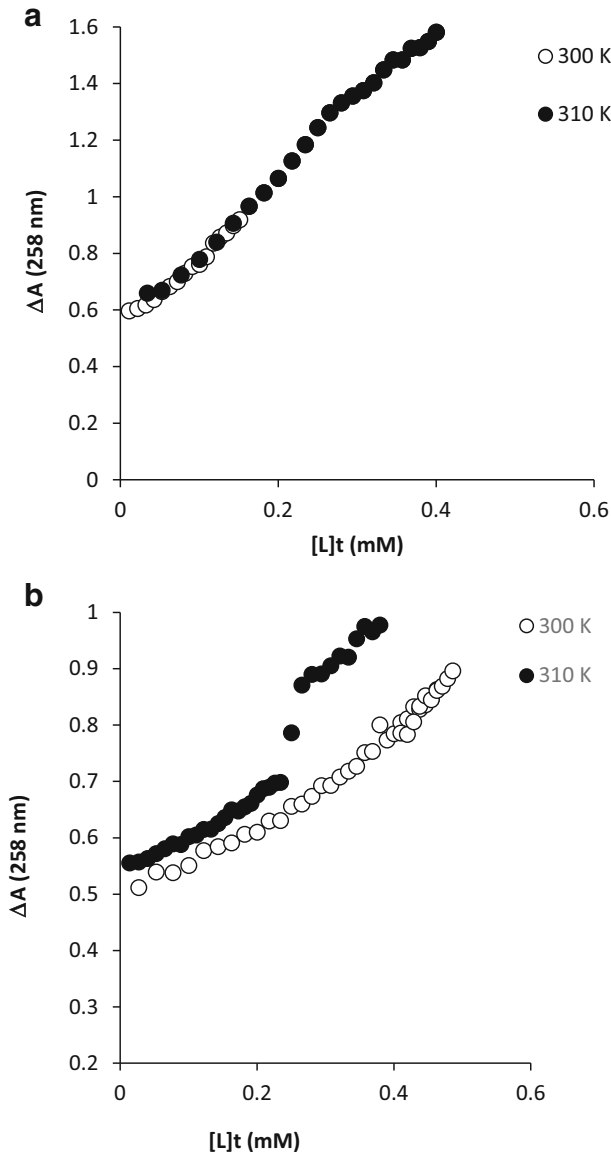


Fig. 1 The changes of absorbance of DNA at $\lambda_{\max} = 258$ nm due to increasing total concentration of cis-[Pt(NH₃)₂(CH₃-gly)]NO₃ insert with cis-[Pt(NH₂-CH₃)₂(CH₃-gly)]NO₃ complex in (o) 300 and (•) 310 K

to 310 K temperature by using the Gibbs-Helmholtz equation as follows [29]:

$$\Delta H^{\circ} = (\Delta G^{\circ}_{T_1}/T_1 - \Delta G^{\circ}_{T_2}/T_2) / (1/T_1 - 1/T_2) \quad (3)$$

On plotting the value of these enthalpies against the concentration of each Pt(II) complex, straight lines will be obtained which are shown in Fig. 3 for cis-[Pt(NH₃)₂(CH₃-gly)]NO₃ and insert for cis-[Pt(NH₂-CH₃)₂(CH₃-gly)]NO₃ complex. Interpolation of these lines (interception

Table 1 Thermodynamic parameters of CT-DNA denaturation by cis-[Pt(NH₃)₂(CH₃-gly)]NO₃ and cis-[Pt(NH₂-CH₃)₂(CH₃-gly)]NO₃

Compound	Temperature (K)	^a <i>m</i> (kJ/mol) (mmol/L) ⁻¹	^b ΔG° _(H₂O) (kJ/mol)	^c ΔH° _(H₂O) (kJ/mol)	^d ΔS° _(H₂O) (kJ/molK)
cis-[Pt(NH ₃) ₂ (CH ₃ -gly)]NO ₃	300	44.3	10.3	561.5	1.83
	310	63.1	28.5		1.71
cis-[Pt(NH ₂ -CH ₃) ₂ (CH ₃ -gly)]NO ₃	300	52.3	25.9	673.7	2.15
	310	63.1	20.4		2.11

^a Ability of platinum complex to denature DNA(kJ/mol) (mmol/L)⁻¹

^b Conformational stability of DNA in the absence of platinum complex (kJ/mol)

^c The heat needed for DNA denaturation in the absence of platinum complex(kJ/mol)

^d The entropy of DNA denaturation by platinum complex(kJ/molK)

ordinate in absence of each metal complex) gives the value of ΔH°_(H₂O) (Table 1). These plots show that in the range of 300 to 310 K changes in enthalpies in the presence of cis-[Pt(NH₃)₂(CH₃-gly)]NO₃ and cis-[Pt(NH₂-CH₃)₂(CH₃-gly)]NO₃ are descending.

The observation indicates that an increase in the concentration of Pt(II) complexes decreases the stability of DNA. In addition, it can be concluding that the interaction both cis-[Pt(NH₃)₂(CH₃-gly)]NO₃ and cis-[Pt(NH₂-CH₃)₂(CH₃-gly)]NO₃ complex with DNA are spontaneous and exothermic. Moreover, the entropy of DNA unfolding by Pt(II) complex, ΔS°_(H₂O), has been calculated using equation, ΔG° = ΔH° - TΔS°, and the data are given in Table 1. These data show that Pt(II)-DNA complex is more disordered than the native DNA, because the entropy changes are positive for both cis-[Pt(NH₃)₂(CH₃-gly)]NO₃ and cis-[Pt(NH₂-CH₃)₂(CH₃-gly)]NO₃ complex in the denaturation process of CT-DNA [30].

Thermal Denaturation (T_m) Studies

Due to raising temperature of DNA solution, the double-stranded DNA gradually dissociated into single strand. T_m is considered as the temperature where half of the total base pairs of DNA are pairs [31]. Thermal behavior of DNA in the presence of complex can give deep insight into their basic conformational changes when temperature is raised and offer information about interaction strength of complexes with DNA. The stabilization of CT-DNA through the groove bonding and electrostatic interactions of the noncovalent complex was carefully assessed by measuring the melting temperature [32].

This experiment was carried out for CT-DNA (0.13 mM) in the absence and presence of 0.108 mM of cis-[Pt(NH₃)₂(CH₃-gly)]NO₃ or cis-[Pt(NH₂-CH₃)₂(CH₃-gly)]NO₃ complex. The melting plot of DNA was monitored by plotting the UV maximum absorption of DNA at 258 nm vs various temperature. T_m of CT-DNA in the absence of complex has been found to be 78 °C. Increasing of DNA melting temperature by 2° for cis-[Pt(NH₃)₂(CH₃-gly)]NO₃ and cis-[Pt(NH₂-CH₃)₂(CH₃-gly)]NO₃ were observed, separately (see Fig. 4). The values show clearly that Pt(II) complexes are able to stabilize DNA helix through non-intercalation mode [33].

Fluorescence Spectroscopic Studies

Cis-[Pt(NH₃)₂(CH₃-gly)]NO₃ and cis-[Pt(NH₂-CH₃)₂(CH₃-gly)]NO₃ are non-fluorescent on excitation invisible region. So, competitive binding studies using ethidium bromide

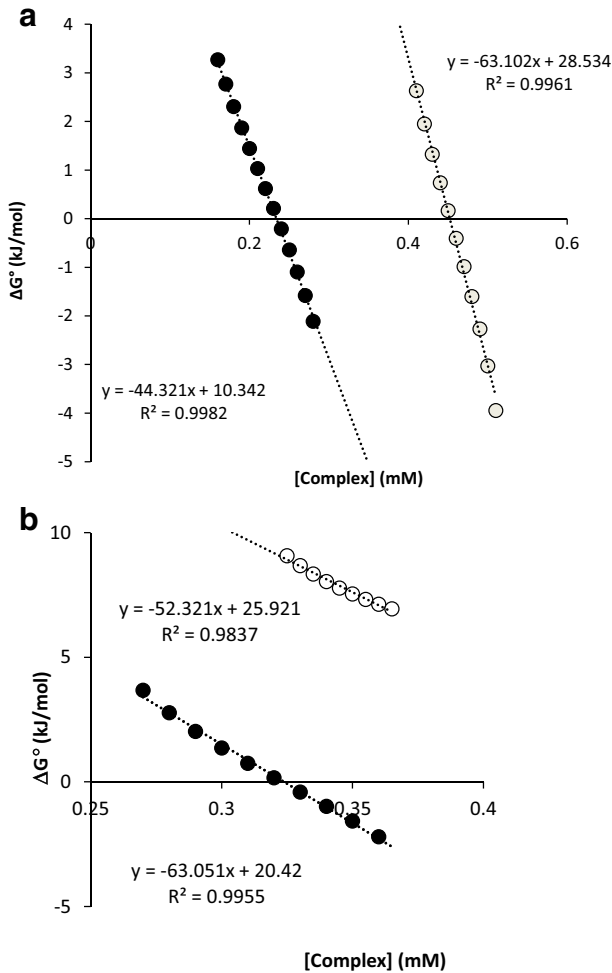


Fig. 2 The molar Gibbs free energy plot of unfolding (ΔG° vs. $[L]_i$) of the CT-DNA in the presence of **a** cis-[Pt(NH₃)₂(CH₃-gly)]NO₃ and **b** cis-[Pt(NH₂-CH₃)₂(CH₃-gly)]NO₃ complex

(EtBr) bound to CT-DNA were carried out for two systems. Ethidium bromide, a fantastic cationic dye, is used widely as a probe for native DNA [34]. The fluorescence intensity of free EtBr is very weak but it is strongly enhanced when EtBr intercalated with DNA base pairs. The quenching extent of fluorescence of EtBr bound to CT-DNA is usually used to determine the mode of binding between the second molecule and CT-DNA. The emission spectra of EtBr-DNA in the absence and the presence of cis-[Pt(NH₃)₂(CH₃-gly)]NO₃ and cis-[Pt(NH₂-CH₃)₂(CH₃-gly)]NO₃ are given in Fig. 5. Gradual reduction emission intensity can be seen by adding different concentrations of each complex when ethidium is removed from duplexes of DNA and released to buffer medium by the action of Pt(II) complex [35].

It has been reported that there are two quenching mechanism of binding quencher-macromolecules: statistic and dynamic quenching. Statistic generally offer formation of a non-

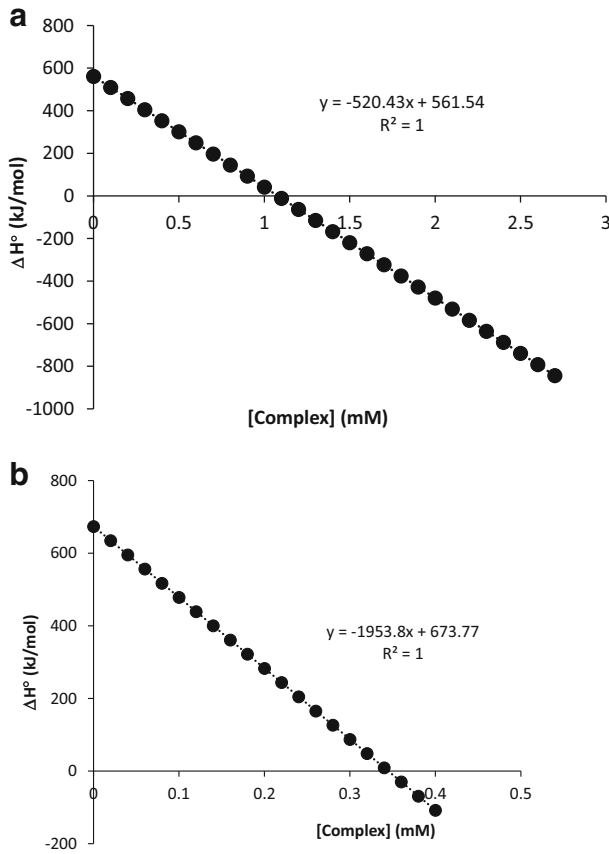


Fig. 3 Plots of molar enthalpies of CT-DNA denaturation ($\Delta H^\circ_{\text{conformation}}$) in the interaction of **a** cis-[Pt(NH₃)₂(CH₃-gly)]NO₃ and **b** cis-[Pt(NH₂-CH₃)₂(CH₃-gly)]NO₃ complex in the range of 300 to 310 K

fluorescent fluorophore quencher complex and the dynamic quenching lead to diffuse the fluorophore during the lifetime of the excited state and the fluorophore returns to ground state without emission of a photon.

To determine the quenching mechanism, the Stern-Volmer is often applied:

$$\frac{F_0}{F} = 1 + k_q \tau_0 [Q] = 1 + K_{sv} \quad (4)$$

where F_0 and F are the fluorescence intensity of CT-DNA in the absence and presence of quencher (here cis-[Pt(NH₃)₂(CH₃gly)]NO₃ and cis-[Pt(NH₂-CH₃)₂(CH₃gly)]NO₃, respectively) and k_q is the EtBr-DNA-Pt(II) complex quenching rate constant; τ_0 is the average lifetime of the fluorophore in the absence of Pt(II) complex as a quencher and the value of fluorescence lifetime of the biopolymer is between 10^{-7} and 10^{-9} s⁻¹. The plot of F_0/F versus $[Q]$ for Pt(II) complexes yielded a linear graph (Fig. 6). $[Q]$ is the total concentration of the quencher. K_{sv} is the linear Stern-Volmer quenching constant [15, 36]. Results are summarized in Table 2.

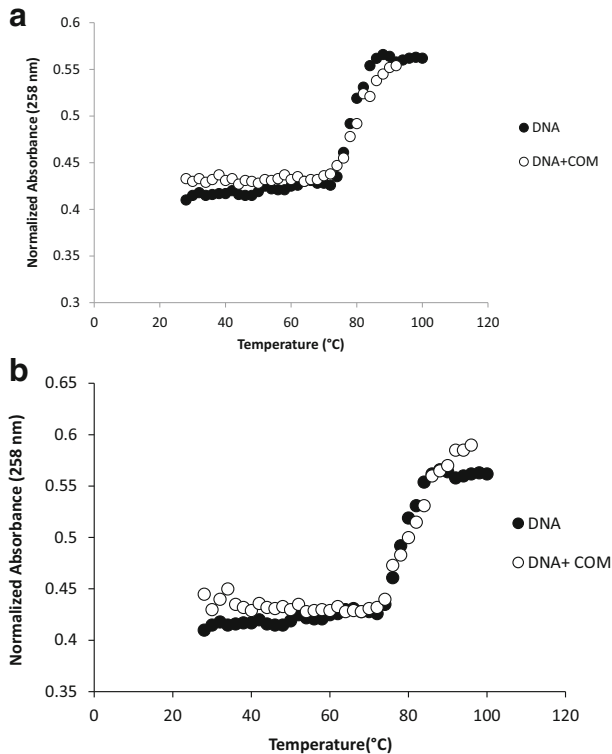


Fig. 4 Melting curves of CT-DNA (1 mM) in the absence and presence of **a** $\text{cis-[Pt(NH}_3)_2(\text{CH}_3\text{-gly)]NO}_3$ and **b** $\text{cis-[Pt(NH}_2\text{-CH}_3)_2(\text{CH}_3\text{-gly)]NO}_3$ complex

Circular Dichroism Spectral Studies

CD technique gives us useful information on how the conformation of DNA is influenced by binding of complex to DNA. The CD spectrum of CT-DNA exhibits a positive band effect at 275 nm due to base stacking and a negative band effect at 245 nm due to the helicity of B-DNA form [23].

The CD spectrum of CT-DNA shows conformational changes by both $\text{cis-[Pt(NH}_3)_2(\text{CH}_3\text{-gly)]NO}_3$ and $\text{cis-[Pt(NH}_2\text{-CH}_3)_2(\text{CH}_3\text{-gly)]NO}_3$ complexes titrations (Fig. 7). In CD spectra for both DNA-Pt(II) complex systems, intensity shift of the negative band to the positive level at 245 nm was observed, while the positive band at 275 nm is increased to higher value. This suggests that DNA binding with Pt(II) complexes induce certain conformational changes, such as the conversion from a model B-like to A-like structure within the DNA molecules. DNA is not a rigid molecule and water molecules are playing an important role on the conformation of DNA. The major and minor grooves are coated by a molecular layer of water molecules with exposed -C=O , -N and -NH functions of glycine in Pt(II) complex structure. The interaction of Pt(II) complexes

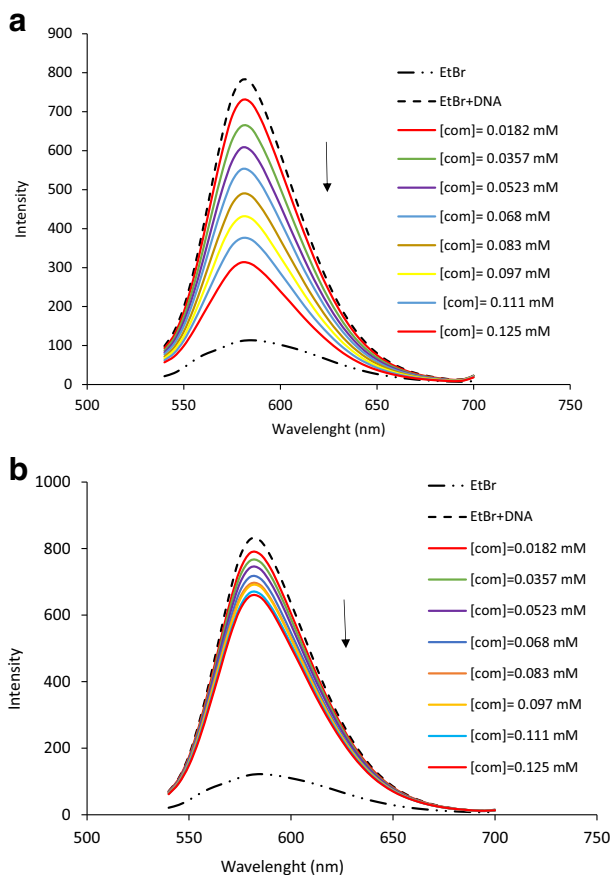


Fig. 5 Fluorescence emission spectra of interacted EtBr-DNA in the absence and presence of different concentration of **a** $\text{cis-[Pt(NH}_3)_2(\text{CH}_3\text{gly)]NO}_3$ and **b** $\text{cis-[Pt(NH}_2\text{-CH}_3)_2(\text{CH}_3\text{gly)]NO}_3$

with minor groove of DNA were occurred with competition between water molecules that solvated the DNA. So, water content in the microsurrounding around the DNA may be decreased and the conformational change may be due to stronger hydrogen binding from B-like to A-like and at A-like in platinum binding [17, 37].

Docking Results

Autodock software moves a molecule or drug around the receptor such as protein, enzyme, DNA, or the other macromolecules randomly based on genetic and Lamarckian algorithm. The basic theory of docking software is molecular mechanic and their force fields are same as molecular dynamics software. So, the molecules translate in the box around the macromolecules. The box is divided by several smaller boxes as grid. Whenever number of grid becomes

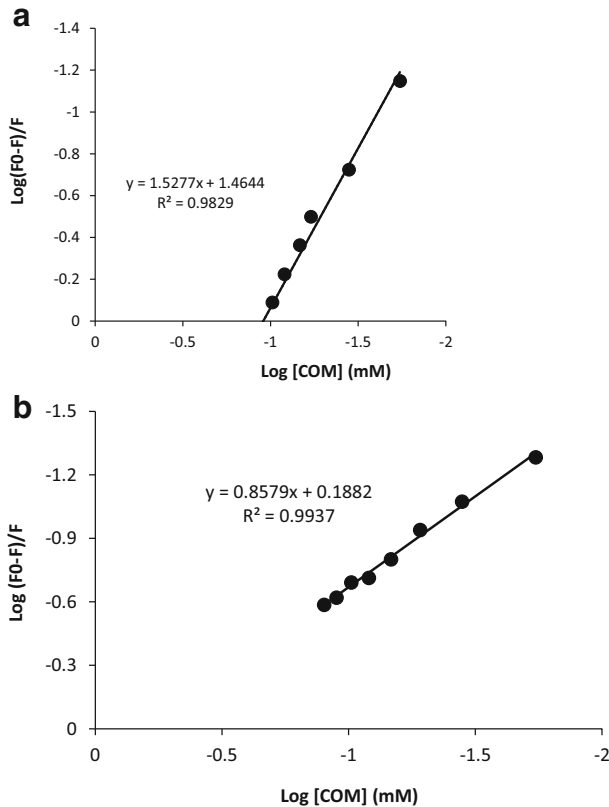


Fig. 6 Plots of $\log(F_0-F)/F$ against $\log[\text{complex}]$ for **a** $\text{cis-}[\text{Pt}(\text{NH}_3)_2(\text{CH}_3\text{gly})]\text{NO}_3$ and **b** $\text{cis-}[\text{Pt}(\text{NH}_2\text{-CH}_3)_2(\text{CH}_3\text{gly})]\text{NO}_3$ quenching effect on EtBr-DNA fluorescence at room temperature

higher and grid size becomes smaller, then results will be more precise, but spend more computer time. All docking parameters were determined by the above-mentioned method. In this study, 500 docking sites were obtained and sorted based on their energies (Table 3). Some of docking sites are located near each other and so form a cluster. The cluster ranks are listed in Table 3. First column is related to cluster rank and the first cluster is the most negative rank. Second column is related to the most negative docking energies and column 3 is related to mean dock energy, and last column is the number of conformation with approximately similar energies in a cluster. The cluster rank 1 has the most population in a cluster and most probable docking site [13, 38]. In comparison of (a) $\text{cis-}[\text{Pt}(\text{NH}_3)_2(\text{CH}_3\text{gly})]\text{NO}_3$ as Pt₁ and (b) $\text{cis-}[\text{Pt}(\text{NH}_2\text{-CH}_3)_2(\text{CH}_3\text{gly})]\text{NO}_3$ complexes as Pt₂, it is observed that the docking energy of Pt₂ is more negative than that of Pt₁, while it is compatible with experimental results. In order to find the molecular basis of this difference, docking sites of both Pt complexes were analyzed.

Figure 8 shows DNA structure which is taken from protein data bank 453D (www.rcsb.org). The 12 cluster ranks also are observed in Fig. 8a as yellow for Pt₁ and blue for Pt₂. Figure 8b shows the docking site of first cluster rank that is located in minor groove.

Table 2 Binding parameters of CT-DNA interaction with cis-[Pt(NH₃)₂(CH₃gly)]NO₃ and cis-[Pt(NH₂-CH₃)₂(CH₃gly)]NO₃ complex obtained from the Stern-Volmer equation

Compound	^a $K_{SV} \times 10^{-3} (M^{-1})$	^b $k_q \times 10^{13} (Ms)^{-1}$	R^2	^c $K_b \times 10^4 (M^{-1})$	n	R^2
cis-[Pt(NH ₃) ₂ (CH ₃ gly)]NO ₃	9.48	9.48	0.97	29.13	1.52	0.99
cis-[Pt(NH ₂ CH ₃) ₂ (CH ₃ gly)]NO ₃	1.98	1.98	0.99	1.54	0.85	0.98

^a K_{SV} is the Stern-Volmer quenching constant

^b k_q is the quenching constant

^c K_f is the binding constant

Both complexes occupied the same site and approximately overlap on each other. Figure 8c confirms our claim that two Pt complexes are located in one position. Label of nearest nucleotide and number of hydrogen bond (green line color) were also shown. As seen from this hydrogen bond for both complexes shown in Fig. 8d, e, there are four hydrogen bonds. In order to know the molecular level difference between two complexes, the thermodynamic parameters were compared in Table 4. The results show that the van der Waals, hydrogen bond, and desolvation energy are more effective than that of electrostatic interactions [39].

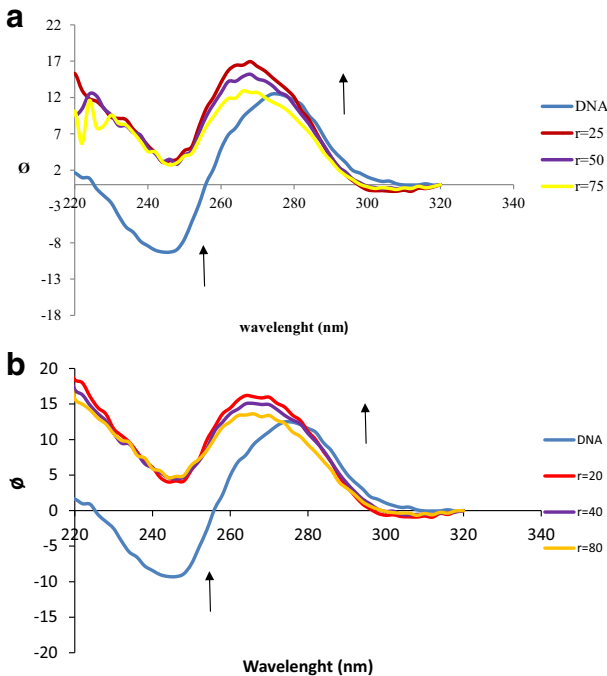


Fig. 7 Circular dichroism Spectra of DNA (1×10^{-3} M) in the absence and presence of increasing amount of (a) cis-[Pt(NH₃)₂(CH₃gly)]NO₃ and (b) cis-[Pt(NH₂-CH₃)₂(CH₃gly)]NO₃ with ratio of $r = [com]/[DNA]$

Table 3 Binding energies (in kcal/mol) obtained by Autodock 4.2

Cluster rank	Lowest binding energy	Mean binding energy	Number of conformations in the cluster
Pt ₁			
0	-7.07	-6.99	334
2	-6.94	-6.90	9
3	-6.87	-6.79	19
4	-6.87	-6.83	26
5	-6.80	-6.80	1
6	-6.77	-6.75	39
7	-6.73	-6.65	25
8	-6.72	-6.65	38
9	-6.64	-6.63	4
10	-6.63	-6.63	1
11	-6.46	-6.46	1
12	-6.45	-6.44	3
Pt ₂			
1	-7.33	-7.17	402
2	-7.22	-7.20	35
3	-7.02	-6.78	13
4	-6.98	-6.90	10
5	-6.96	-6.90	11
6	-6.94	-6.93	3
7	-6.84	-6.70	5
8	-6.82	-6.80	9
9	-6.82	-6.80	2
10	-6.79	-6.76	2
11	-6.75	-6.65	7
12	-6.71	-6.71	1

Cytotoxicity Studies of Pt(II) Complexes

The anticancer and growth inhibitory activity of the two new synthesized complexes of *cis*-[Pt(NH₃)₂(CH₃gly)]NO₃ and *cis*-[Pt(NH₂-CH₃)₂(CH₃gly)]NO₃ were investigated against human model breast cancer cell line of MCF7 using MTT assay. Human breast adenocarcinoma cancer model cell line of MCF7 was incubated with various concentrations of both complexes ranging from 0 to 350 μM (Fig. 9). According to the results (Fig. 9), the 50% cytotoxic concentrations (C_{c50}) of the complexes were calculated 126 and 292 μM for complexes of *cis*-[Pt(NH₃)₂(CH₃gly)]NO₃ and *cis*-[Pt(NH₂-CH₃)₂(CH₃gly)]NO₃, respectively, after 24 h incubation time.

The effects of synthesized Pt(II) complexes on the morphological features of human cancer cell line of MCF7 (Fig. 10 from left to right, incubated in the absence of complex or control, and in the presence of *cis*-[Pt(NH₃)₂(CH₃-gly)]NO₃ and *cis*-[Pt(NH₂-CH₃)₂(CH₃-gly)]NO₃) were studied using phase-contrast microscopy. Phase-contrast microscopy results have shown a decreasing in cell density in the presence of complexes relative control image. Also, the results indicated cell rounding and shrinking in the presence of complexes. Also, cytotoxicity results show that the presence of the methyl groups and increasing of lipophilicity of cisplatin analog have reverse influence on the growth suppression activity of the complex on MCF7 cells and cause more C_{c50} value of *cis*-[Pt(NH₂-CH₃)₂(CH₃gly)]NO₃ complex.

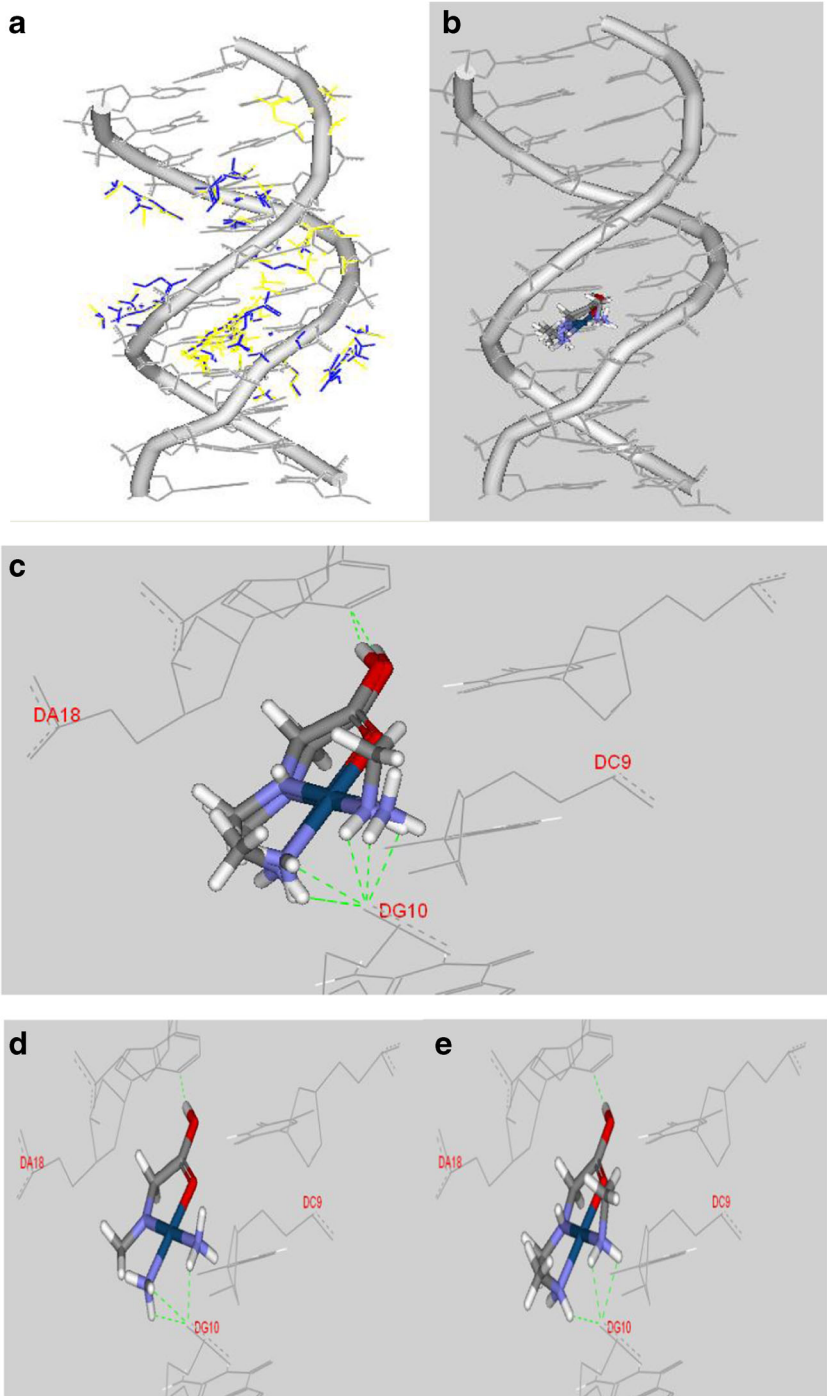


Fig. 8 (a) Structure of DNA taken from protein data bank (453D) (b) binding sites of two platinum complexes (c) binding site of 12 cluster ranks (d) binding site of the most negative cluster rank, first cluster rank in Table 3 (e) zoom structure and nearest nucleotide around the complex

Table 4 Thermodynamic parameters for the most negative cluster rank (rank 1 in Table 3) for two platinum complexes

Thermodynamic parameters (kcal/mol)	cis-[Pt(NH ₃) ₂ (CH ₃ -gly)]NO ₃	cis-[Pt(NH ₂ CH ₃) ₂ (CH ₃ gly)]NO ₃
Estimated free energy of binding	-7.07	-7.17
Estimated inhibition constant, K_i	6.59 μ M	5.59 μ M
Final intermolecular energy	-7.62	-7.71
vdW + Hbond + desolv energy	-3.29	-3.75
Electrostatic energy	-4.33	-3.97
Final total internal energy	+0.84	+0.58
Torsional free energy	+0.55	+0.50
Unbound system's energy	+0.84	+0.58

Conclusion

In the present study, two new created and water-soluble compounds, cis-[Pt(NH₃)₂(CH₃gly)]NO₃ and cis-[Pt(NH₂-CH₃)₂(CH₃gly)]NO₃, were synthesized and characterized by spectroscopic techniques as IR, ¹H NMR, UV-Vis, and elemental analysis. Cytotoxic data show that the C₅₀ value of cis-[Pt(NH₃)₂(CH₃gly)]NO₃ is lower than that of cis-[Pt(NH₂-CH₃)₂(CH₃gly)]NO₃ complex which indicate more cytotoxicity and anticancer activity for this compound. According to spectroscopic results, cis-[Pt(NH₃)₂(CH₃gly)]NO₃ and cis-[Pt(NH₂-CH₃)₂(CH₃gly)]NO₃ complexes can bind to CT-DNA by groove binding. Different instrumental methods were used to the investigation of the interaction modes. Determinations of several binding and thermodynamic

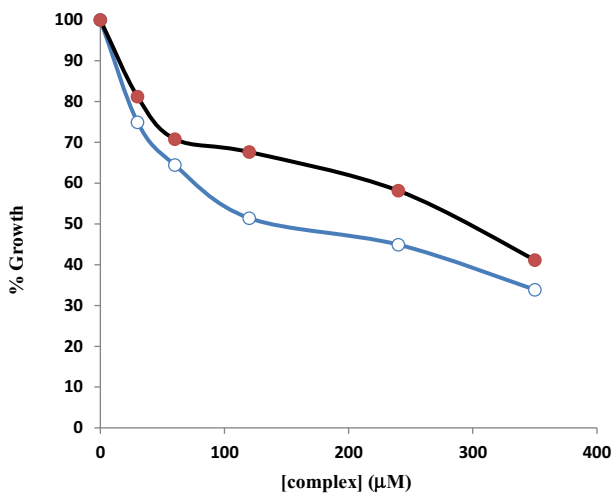


Fig. 9 The growth inhibitory activity of the complexes of cis-[Pt(NH₃)₂(CH₃gly)]NO₃ (O) and cis-[Pt(NH₂-CH₃)₂(CH₃gly)]NO₃ (•) on breast cancer line of MCF7; incubated with varying concentrations of the complexes for 24 h using MTT assay

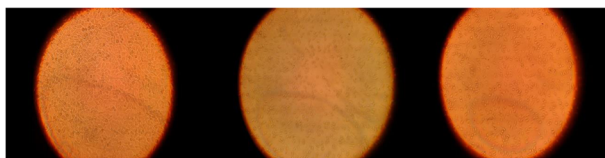


Fig. 10 Phase-contrast microscopy of the effects of synthesized Pt(II) complexes on the morphological features of human cancer cell line of MCF7 (from left to right, incubated in the absence of complex or control, in the presence of cis-[Pt(NH₃)₂(CH₃-gly)]NO₃ and cis-[Pt(NH₂-CH₃)₂(CH₃-gly)]NO₃)

parameters have also been attempted. Overall, experimental results indicate that the interaction affinity of cis-[Pt(NH₂-CH₃)₂(CH₃-gly)]NO₃ is more than that of cis-[Pt(NH₃)₂(CH₃-gly)]NO₃ complex analog. It is hoped that current study will open the new approaches for the development of efficient pharmaceutical systems in cancer treatment with low cytotoxic effects.

Acknowledgments The Research Council of Chemistry & Chemical Engineering Research Center of Iran is gratefully acknowledged for supporting this work.

Compliance with Ethical Standards

Conflict of Interest The authors declare that they have no conflict of interest.

References

- Weaver, A., Flemming, S., Kish, J., Vandenberg, H., Jacob, J., Crissman, J., & Al-Sarraf, M. (1982). Cis-platinum and 5-fluorouracil as induction therapy for advanced head and neck cancer. *The American Journal of Surgery*, *144*(4), 445–448.
- Storr, T., Thompson, K. H., & Orvig, C. (2006). Design of targeting ligands in medicinal inorganic chemistry. *Chemical Society Reviews*, *35*(6), 534–544.
- Farrell, N. (2015). Multi-platinum anti-cancer agents. Substitution-inert compounds for tumor selectivity and new targets. *Chemical Society Reviews*, *44*(24), 8773–8785.
- Deubel, D. V. (2004). Factors governing the kinetic competition of nitrogen and sulfur ligands in cisplatin binding to biological targets. *Journal of the American Chemical Society*, *126*(19), 5999–6004.
- Yousefi, R., Aghevlian, S., Mokhtari, F., Samouei, H., Rashidi, M., Nabavizadeh, S. M., Tavaf, Z., Pouryasyn, Z., Niazi, A., Faghghi, R., & Papari, M. M. (2012). The anticancer activity and HSA binding properties of the structurally related platinum (II) complexes. *Applied Biochemistry and Biotechnology*, *167*(4), 861–872.
- Barabas, K., Milner, R., Lurie, D., & Adin, C. (2008). Cisplatin: a review of toxicities and therapeutic applications. *Veterinary and Comparative Oncology*, *6*(1), 1–18.
- Wu, G. (2009). Amino acids: metabolism, functions, and nutrition. *Amino Acids*, *37*(1), 1–17.
- Gentilucci, L., De Marco, R., & Cerisoli, L. (2010). Chemical modifications designed to improve peptide stability: incorporation of non-natural amino acids, pseudo-peptide bonds, and cyclization. *Current Pharmaceutical Design*, *16*(28), 3185–3203.
- Zhao, M., Yang, M., Li, X.-M., Jiang, P., Baranov, E., Li, S., & Hoffman, R. M. (2005). Tumor-targeting bacterial therapy with amino acid auxotrophs of GFP-expressing *Salmonella typhimurium*. *Proceedings of the National Academy of Sciences of the United States of America*, *102*(3), 755–760.
- Gorre, M. E., Mohammed, M., Ellwood, K., Hsu, N., Paquette, R., Rao, P. N., & Sawyers, C. L. (2001). Clinical resistance to STI-571 cancer therapy caused by BCR-ABL gene mutation or amplification. *Science*, *293*(5531), 876–880.

11. Eslami Moghadam, M., Saidifar, M., Divsalar, A., Mansouri-Torshizi, H., Saboury, A. A., Farhangian, H., & Ghadamgahi, M. (2016). Rich spectroscopic and molecular dynamic studies on the interaction of cytotoxic Pt (II) and Pd (II) complexes of glycine derivatives with calf thymus DNA. *Journal of Biomolecular Structure and Dynamics*, *34*(1), 206–222.
12. Safa Shams Abyaneh, F., Eslami Moghadam, M., Hoseini Sadr, M., & Divsalar, A. (2017). Effect of lipophilicity of amylamine and amyglycine ligands on biological activity of new anticancer cisplatin analog. *Journal of Biomolecular Structure and Dynamics*, 1–13. <https://doi.org/10.1080/07391102.2017.1301273>.
13. Ajloo, D., Moghadam, M. E., Ghadimi, K., Ghadamgahi, M., Saboury, A. A., Divsalar, A., & Yousefi, K. (2015). Synthesis, characterization, spectroscopy, cytotoxic activity and molecular dynamic study on the interaction of three palladium complexes of phenanthroline and glycine derivatives with calf thymus DNA. *Inorganica Chimica Acta*, *430*, 144–160.
14. Kantoury, M., Eslami Moghadam, M., Tarlani, A. A., & Divsalar, A. (2016). Structure effect of some new anticancer Pt (II) complexes of amino acid derivatives with small branched or linear hydrocarbon chains on their DNA interaction. *Chemical Biology & Drug Design*, *88*(1), 76–87.
15. Heydari, M., Moghadam, M. E., Tarlani, A., & Farhangian, H. (2017). DNA as a target for anticancer phenimidazole Pd (II) complexes. *Applied Biochemistry and Biotechnology*, *182*(1), 110–127.
16. Lippert, B. (1999). *Cisplatin: chemistry and biochemistry of a leading anticancer drug*. Zürich: John Wiley & Sons, Verlag Helvetica Chimica Acta.
17. Hadian Rasanani, S., Eslami Moghadam, M., Soleimani, E., Divsalar, A., & Tarlani, A. (2017). Improving activity of anticancer oxalipalladium analog by the modification of oxalate group with isopentylglycine. *Journal of Coordination Chemistry*, *70*(22), 3769–3789.
18. Eslami Moghadam, M., Divsalar, A., Abolhosseini Shahrmoay, A., & Saboury, A. A. (2016). Synthesis, cytotoxicity assessment, and interaction and docking of novel palladium (II) complexes of imidazole derivatives with human serum albumin. *Journal of Biomolecular Structure and Dynamics*, *34*(8), 1751–1762.
19. Mansouri-Torshizi, H., Shahraki, S., Nezami, Z. S., Ghahghaei, A., Najmedini, S., Divsalar, A., Ghaemi, H., & Saboury, A.-A. (2014). Platinum (II)/palladium (II) complexes with n-propyldithiocarbamate and 2, 2'-bipyridine: synthesis, characterization, biological activity and interaction with calf thymus DNA. *Complex Metals*, *1*(1), 23–31.
20. Yakovchuk, P., Protozanova, E., & Frank-Kamenetskii, M. D. (2006). Base-stacking and base-pairing contributions into thermal stability of the DNA double helix. *Nucleic Acids Research*, *34*(2), 564–574.
21. Mansouri-Torshizi, H., Saeidifar, M., Divsalar, A., & Saboury, A. A. (2010). Interaction studies between a 1, 10-phenanthroline adduct of palladium (II) dithiocarbamate anti-tumor complex and calf thymus DNA. A synthesis spectral and in-vitro study. *Spectrochimica Acta Part A: Molecular and Biomolecular Spectroscopy*, *77*(1), 312–318.
22. Shahabadi, N., Kashanian, S., & Darabi, F. (2009). In vitro study of DNA interaction with a water-soluble dinitrogen Schiff base. *DNA and Cell Biology*, *28*(11), 589–596.
23. Macquet, J. P., & Butour, J. L. (1978). A circular dichroism study of DNA· platinum complexes. *The FEBS Journal*, *83*(2), 375–387.
24. Sullivan, E. (1979). Circular dichroism of palladium (II) and platinum (II) diamine complexes. *Canadian Journal of Chemistry*, *57*(1), 67–70.
25. Ajloo, D., Yoonesi, B., & Soleymannpour, A. (2010). Solvent effect on the reduction potential of anthraquinones derivatives. The experimental and computational studies. *International Journal of Electrochemical Science*, *5*, 459–477.
26. Saeidifar, M., Mansouri-Torshizi, H., Palizdar, Y., Divsalar, A., & Saboury, A. A. (2013). Synthesis, characterization, and cytotoxicity studies of a novel palladium (II) complex and evaluation of DNA-binding aspects. *Nucleosides, Nucleotides and Nucleic Acids*, *32*(7), 366–388.
27. Shahraki, S., Mansouri-Torshizi, H., Heydari, A., Ghahghaei, A., Divsalar, A., Saboury, A., et al. (2015). Platinum (II) and palladium (II) complexes with 1, 10-phenanthroline and pyrrolidinedithiocarbamate ligands: synthesis, DNA-binding and anti-tumor activity in leukemia K562 cell lines. *Iranian Journal of Science and Technology*, *39*(A2), 187.
28. Aminzadeh, M., Mansouri-Torshizi, H., & Modarresi-Alam, A. R. (2016). 2, 2'-bipyridine coplanar with coordination square of Pd (II) nonyldithiocarbamate antitumor complex interacting with DNA in two distinct steps. *Journal of Biomolecular Structure and Dynamics*, *35*, 1–13.
29. Saeidifar, M., Mansouri-Torshizi, H., Palizdar, Y., Eslami-Moghaddam, M., Divsalar, A., & Saboury, A. A. (2014). Synthesis, characterization, cytotoxicity and DNA binding studies of a novel anionic organopalladium (II) complex. *Acta Chimica Slovenica*, *61*(1), 126–136.
30. Mansouri-Torshizi, H., Saeidifar, M., Khosravi, F., Divsalar, A., Saboury, A. A., & Hassani, F. (2011). DNA binding and antitumor activity of α -diimineplatinum (II) and palladium (II) dithiocarbamate complexes. *Bioinorganic Chemistry and Applications*, *2011*, 1–11.

31. Marmur, J., & Doty, P. (1962). Determination of the base composition of deoxyribonucleic acid from its thermal denaturation temperature. *Journal of Molecular Biology*, 5(1), 109–118.
32. Mansouri-Torshizi, H., Saeidifar, M., Divsalar, A., & Saboury, A. (2011). Study on interaction of DNA from calf thymus with 1, 10-phenanthrolinehexyldithiocarbamatopalladium (II) nitrate as potential antitumor agent. *Journal of Biomolecular Structure and Dynamics*, 28(5), 805–814.
33. Shahabadi, N., Kashanian, S., & Purfoulad, M. (2009). DNA interaction studies of a platinum (II) complex, PtCl₂ 2 (NN)(NN= 4, 7-dimethyl-1, 10-phenanthroline), using different instrumental methods. *Spectrochimica Acta Part A: Molecular and Biomolecular Spectroscopy*, 72(4), 757–761.
34. Ware, W. R. (1962). Oxygen quenching of fluorescence in solution: an experimental study of the diffusion process. *The Journal of Physical Chemistry*, 66(3), 455–458.
35. Shahabadi, N., Maghsudi, M., Mahdavi, M., & Pourfoulad, M. (2012). Interaction of calf thymus DNA with the antiviral drug lamivudine. *DNA and Cell Biology*, 31(1), 122–127.
36. Ghalandari, B., Divsalar, A., Eslami-Moghadam, M., Saboury, A. A., Haertlé, T., Amanlou, M., & Parivar, K. (2015). Probing of the interaction between β -lactoglobulin and the anticancer drug oxaliplatin. *Applied Biochemistry and Biotechnology*, 175(2), 974–987.
37. Mostafavinia, S. E., & Hoshyar, R. (2016). Spectroscopic studies on the interaction of anticancer rosemary with ctDNA. *Gene, Cell and Tissue*, 3(2), e35638.
38. Lang, P. T., Brozell, S. R., Mukherjee, S., Pettersen, E. F., Meng, E. C., Thomas, V., Rizzo, R. C., Case, D. A., James, T. L., & Kuntz, I. D. (2009). DOCK 6: combining techniques to model RNA–small molecule complexes. *RNA*, 15(6), 1219–1230.
39. Arjmand, F., Parveen, S., Afzal, M., & Shahid, M. (2012). Synthesis, characterization, biological studies (DNA binding, cleavage, antibacterial and topoisomerase I) and molecular docking of copper (II) benzimidazole complexes. *Journal of Photochemistry and Photobiology B: Biology*, 114, 15–26.